Flat Structures, Teichmuller theory and Handle Addition for Minimal Surfaces

Michael Wolf*

1 Introduction

The Weierstraß representation is a powerful tool bringing methods of complex analysis to bear on problems of existence in minimal surface theory. It is particularily powerful in constructing minimal surfaces of low genus and few ends, as the problem of ensuring that the resulting representation is well-defined (the so-called "period problem") naturally translates into a problem in a low-dimensional moduli space, which can then be solved either explicitly, or by use of techniques adapted to low-dimensional spaces, like the intermediate value theorem (for one-dimensional spaces).

These latter methods see particular success in the handle-addition theorems of Chen-Gackstatter, Karcher and others ([CG81], [CG82], [HMI90], [HW], [Kar88], [Kar89], [Kar91]). These results beg the question as to how extensively and systematically one can continue to add handles to existing minimal surfaces.

We describe here work with Matthias Weber [1] in which we show an inductive method that adds successive handles (and ends) to known minimal surfaces, producing families of minimal surfaces of increasing complexity. We might *very* informally state the result as

Theorem 1.0.1 (Handle Addition). *(Weber-Wolf) For a number of classes of geometric descriptions of surfaces, there exist families of minimal examples indexed by genus or by genus and number of ends.*

The generality of the result is that the architecture of the proof and many of the components apply to a number of widely varying classes of surfaces, while the particular class of surfaces only affects one (global) choice within the proof.

We now describe the results more carefully, beginning with four sample theorems of the type of Theorem 1.0.1.

Theorem 1.0.2 (Adding Handles to Enneper). *[WW98] For each $g \geq 0$, there is a complete minimal surface E_g in $\mathbb{E}^3$ of genus $g \geq 0$ and one Enneper-type end with total curvature $-2\pi(g+1)$ and eight symmetries.*

This theorem has something of a long history: the original surface is due to Enneper [Enn69], and then one and two handles were added by Chen-Gackstatter [CG82]. A surface with an Enneper-type end and genus three was found by d'Espirito-Santo [San94], and then shortly afterwards, Thayer displayed convincing numerical evidence of the existence of surfaces of this type for all genera $g \leq 35$ [Tha94]. For arbitrary genus, the result above was independently obtained by Sato [Sat96].

Even though these surfaces are not embedded, they are perhaps still interesting: the surface E_g minimizes, among all complete immersed minimal surfaces of genus g, the degree of the Gauss map (i.e. maximizes the total curvature). (by Jorge-Meeks [JI83] inequality). An example of these surfaces is drawn in Figure 6.

*Partially supported by NSF grant DMS 9971563

[1] Many of the figures in this paper, including all of the images of minimal surfaces, are due to Matthias Weber.

Theorem 1.0.3 (Adding Handles and Ends to Costa). *[WW] For all odd genera g, there is a complete minimal surface $CT_g \subset \mathbb{E}^3$ which is embedded outside a compact surface with boundary of genus g, with g parallel (horizontal) planar ends and two catenoid ends. The symmetry group of CT_g is generated by reflective symmetries about a pair of orthogonal vertical planes and a rotational symmetry about a horizontal line.*

These surfaces look like

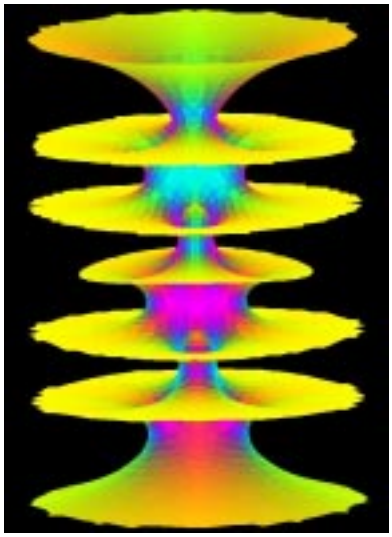

Figure 1: The surface CT_5 of genus 5 with five planar ends and two catenoid ends. One can imagine this as being a desingularization of the intersection of five horizontal planes with a catenoid.

Here one might imagine that the original Costa surface results from desingularizing the intersection of a horizontal surface with a (vertical) catenoid; analogously, these surfaces might result from desingularizing the intersection of an odd number of planes with a catenoid.

We generalize these CT_g surfaces as follows, imagining **D**rilling additional **H**oles to obtain surfaces $DH_{m,n}$.

Theorem 1.0.4 (Adding Handles to CT_g surfaces). (i) *For every pair of integers $n \geq m \geq 1$, there exists a complete minimal surface $DH_{m,n} \subset \mathbb{E}^3$ of genus $m+n+1$ which is embedded outside a compact set with the following properties: it has $2n+1$ vertical normals, $2m+1$ planar ends, and two catenoid ends. The symmetry group is as in Theorem A.* (ii) *For $n < m$, there is no complete minimal surface with those symmetries of the type $DH_{m,n}$ (and $2n+1$ vertical normals, $2m+1$ planar ends, and two catenoid ends).*

What is interesting about Theorem 1.0.4 is how it is consistent with the Hoffman-Meeks conjecture (see [HK97]) that if there exists an embedded minimal surface of genus g with e ends, then $g \geq e-2$. A tabular form of Theorem 1.0.4 looks like

$m\backslash n$	0	1	2	3	4	5	6
0	Costa	Horgan	M-W	?	?	?	?
1	–	B-W	+	+	+	+	+
2	–	–	+	+	+	+	+
3	–	–	–	+	+	+	+
4	–	–	–	–	+	+	+
5	–	–	–	–	–	+	+

This table shows existence (as a "+") and non-existence (as a "-") for surfaces of type (m,n). Here "Costa" refers to the surface announced in [Cos84], "Horgan" refers to the surface discussed in [Web98],

"M-W" refers to the surface discussed in [MW01], and "B-W"refers to the surface of Boix and Wohlgemuth (see [BW]). The surface with $m = n = 2$ is shown in Figure 1, while the surface with $m = 1, n = 2$ is shown in Figure 29 at the end of the article.

The techniques of Theorem 1.0.1 also apply to periodic surfaces; for instance, we can inductively add handles to Scherk's doubly periodic surface. (See Figure 12.)

Theorem 1.0.5 (Adding Handles to Scherk's Doubly Periodic Surface). *[WW01] For each $g \geq 0$, there is a complete doubly-periodic minimal surface S_g in $\mathbb{E}^3$, whose quotient has genus $g \geq 0$ and four planar parallel ends, parallel to the ends of Scherk's doubly periodic surface S_0.*

Weber [Web00] has added handles to the surfaces [CHMI89] of Callahan-Hoffman-Meeks; again the architecture of the proof is identical.

Theorem 1.0.6 (Adding Handles to Callahan-Hoffman-Meeks). *[Web00] For each pair of integers $1 \leq m \leq n$, there is a singly periodic complete minimal surface $CHM_{m,n}$ in $\mathbb{E}^3$ invariant under a translation whose quotient has $2m$ planar ends, genus $m + n + 1$ and eight symmetries.*

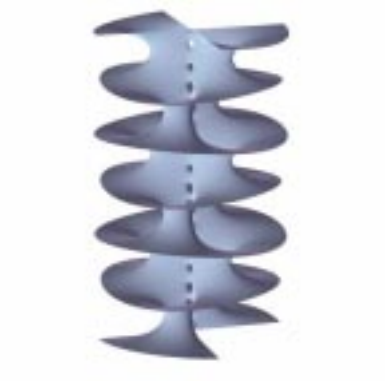

Figure 2: Weber's handle addition to the Callahan-Hoffman-Meeks surface

In this paper, we describe the proofs of these theorems, focusing for the sake of concreteness almost exclusively on the case of the Enneper-ended examples of Theorem 1.0.2. After defining our notation and recalling some background information in that notation in the next section, we give an overview of the method in the third and fourth sections. In these final sections, we focus on each of the steps of the proof, giving some, but not all, of the details of each of the steps of the proofs. Complete proofs may be found in the referenced articles.

2 Background and Notation

2.1 The Weierstraß Representation

Our arguments are founded upon the Weierstraß representation. To set notation, recall that for a minimal surface on whose underlying Riemann surface $\mathcal{R}$ we have a holomorphic function G and a holomorphic form dh (not necessarily exact, despite the notation), the minimal immersion may be represented via a map $\mathcal{R} \to \mathbb{E}^3$ by

$$z \mapsto \mathrm{Re} \int_{\rho_0}^{z} \left(\tfrac{1}{2}\left(G - \tfrac{1}{G}\right) dh, \tfrac{i}{2}\left(G + \tfrac{1}{G}\right) dh, dh \right).$$

For this surface, G will be the Gauss map (postcomposed with stereographic projection) and dh will be the complexified differential of the third coordinate in $\mathbb{E}^3$.

Examples: 1) Enneper's surface (1869) $G = z$, $dh = zdz$ on $\mathcal{R} = \mathbb{C}$. The surfaces for Theorem 1.0.2 have one end asymptotic to the end of this surface.

Figure 3: The Classical Enneper Surface

2) Catenoid: $G = z$, $dh = \frac{dz}{z}$ on $\mathbb{C} - \{0\}$; top and bottom ends of the family for Theorem 1.0.3 are asymptotically catenoids.

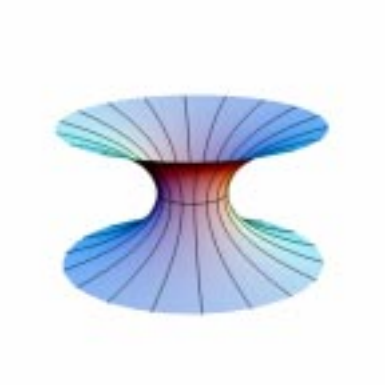

Figure 4: The catenoid

There are, of course, some restrictions on the possible Weierstraß data. To begin, we compute that the metric on $F(\mathcal{R})$ is

$$ds_{F(R)} = \left(|G| + \frac{1}{|G|}\right)|dh|; \tag{2.1.1}$$

thus, to get a regular metric, we need compatible divisors for G and dh at regular points of the surface. This is a pretty mild restriction, as it is all local.

The global problem for producing minimal surfaces is that of well-definedness: continuation around a cycle must leave the map unchanged. Thus we require

$$\begin{aligned} \operatorname{Re}\int_\gamma \tfrac{1}{2}\left(G - \tfrac{1}{G}\right)dh &= \operatorname{Re}\int_\gamma \tfrac{i}{2}\left(G + \tfrac{1}{G}\right)dh \\ &= \operatorname{Re}\int_\gamma dh = 0 \end{aligned} \tag{2.1.2}$$

for every cycle $\gamma \subset \mathcal{R}$.

Rephrasing: We prefer to work with the meromorphic data of two forms Gdh and $\frac{1}{G}dh$. Then we can phrase the **period problem** as

$$\begin{aligned} \int_\gamma Gdh &= \overline{\int_\gamma \tfrac{1}{G}dh} \\ \mathrm{Re}\int_\gamma dh &= 0 \end{aligned} \tag{2.1.3}$$

for every cycle $\gamma \subset \mathcal{R}$.

3 The Geometry of Orthodisks

How should one approach the "period problem"? More generally, how does one picture a period of a one-form on a Riemann surface? For the type of problems we are considering, where the fundamental domain of the desired minimal surface (with respect to the desired symmetry group) is a planar domain, we adopt the perspective that a one-form on a Riemann surface provides for a singular Euclidean structure on the surface.

This is but a global summary of some straightforward local computations. Locally, if $\alpha = f(z)dz$ is a one-form on a Riemann surface $\mathcal{R}$, then we can define a line element ds_α by

$$ds_\alpha = |\alpha| = |f(z)||dz| \tag{3.0.4}$$

Then, away from the zeroes of α, the metric ds_α has curvature

$$K = \frac{-2}{f(z)}\partial\overline{\partial} log f(z) = 0 \tag{3.0.5}$$

since f is meromorphic.

At a zero or pole p of α, by comparing the radius and circumference of small circle about the singularity p, we find that if $\alpha = \{z^k + h.o.t.\}dz$, then ds_α is isometric to a Euclidean cone with cone angle $2\pi(k+1)$ at p.

3.1 Flat Structure Triples

Here's a motivating example (Thurston): Consider a parallelogram in the plane with the usual toral identifications, and its two complementary regions Ω_0 and Ω_∞ in $\hat{\mathbb{C}}$. Consider the one-form dz on each of these regions.

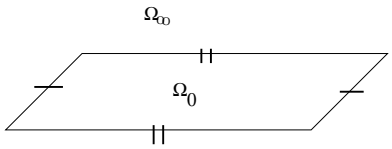

Figure 5: A parallelogram with identifications defines two tori, each with a one-form

With the identifications, each domain is a torus, say T_0 and T_∞, respectively. The one-form dz restricts to be the familiar non-vanishing holomorphic form on T_0, but on T_∞, the one-form dz has a second order pole at ∞, and is regular elsewhere. Thus, this form corresponds to a Weierstraß $\mathfrak{P}$-function (multiplied by the non-vanishing holomorphic one-form) on T_∞. The zero of this form occurs at the vertex of the parallelogram – note the total cone angle there of 6π.

Most significantly, note that here we have two (typically different) Riemann surfaces, each equipped with a one-form so that under a natural correspondence of cycles, the periods of the one-forms are negatives of one another (with the periods understood in terms of Euclidean geometry).

This device of pairs of flat metrics representing pairs of Riemann surfaces and one-forms where the Euclidean geometry of the pairs reflects a relationship between the periods of the one-forms drives all of our constructions.

As we noted in the introduction, when we discuss details in this paper, we will focus on the case of the Enneper-ended surfaces of Theorem 1.0.2. So before going much farther, we now deduce the general forms of the flat structures required for these Enneper-ended surfaces E_g. Since we have the benefit of a computer simulation of some of these surfaces, we can use these images; in general, we would have some image suggested at least by intuition.

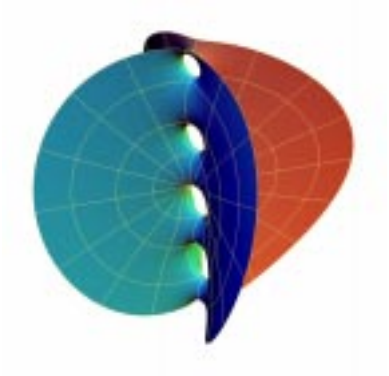

Figure 6: The Chen-Gackstatter Surface with four handles

We begin our analysis using the figure. First, note that this surface has reflections in two vertical planes (as well as one additional symmetry we will discuss somewhat later). Thus, its quotient by the group of reflections will be a planar domain which itself has a symmetry. Next, observe that there are nine points, say $H_1, H_2, \ldots, H_9$ on the central axis where the tangent plane is horizontal. Thus the form dh, which is a component of the Weierstraß data, will have a zero at those points: we need to decide on the order of the zero. The simulation Figure 6 leads us to imagine that this zero is simple, and so we will assume that for the rest of the discussion – remember that at this stage, we are trying to set up a candidate space for proving existence, and so we are free to assume anything we want about that surface we are trying to prove exists. (The peril of this, of course, is that we can restrict our space of candidates too much, and so exclude the actual minimal surface from consideration.) Since these points H_i are on the surface, we will need the induced metric to be regular, and so, from formula 2.1.1, we require that the Gauß map G have either a simple zero or a simple pole at those points.

We look once more at our simulation, and do not observe any other points with a horizontal tangent plane, so we declare that the divisor of the surface is supported on the points H_i and the single end, say E, where our surface is asymptotic to Enneper's original surface. Thus we can read off the relevant Weierstraß data at that point E from the coresponding data at the end of Enneper's surface: we declare that dh should have a third order pole at E, while G should have a simple zero or pole, depending on how we orient the surface.

With these considerations in mind, we can tabulate the Weierstraß data on the divisor of G (or dh) as follows:

	ord dh	ord G
H_1	1	-1
H_2	1	1
H_3	1	-1
H_4	1	1
H_5	1	-1
H_6	1	1
H_7	1	-1
H_8	1	1
H_9	1	-1
E	-3	1

Figure 7: Divisor data for the surface E_4

All of these derivations of divisor data for a Weierstraß representation are quite standard in the theory of minimal surfaces: our next goal is to simplify the appearance of the period problem by converting this data into candidates for the flat structures of the forms Gdh, $\frac{1}{G}dh$ and dh. To do this, we go back to the simulation and make one further observation: the surface meets the four vertical (symmetry) coordinate planes in curves along which G is either purely real or purely imaginary, and for which dh is purely real (this also involves a choice of stereographic projection for the Gauß map). Thus the forms Gdh and $\frac{1}{G}dh$ are either purely real or purely imaginary along those arcs. Thus the image of the one quarter of the surface bounded by the vertical planes will develop onto a region bounded by a polygonal arc with either purely real or purely imaginary line segments.

What are the angles that these segments meet at? Since the segments meet at one of the points H_i or E, this is already determined by the divisor data in the table above. We convert this complex analytic information to geometric data in the next table, using that the cone corresponding to a zero of order k has an angle of $2\pi(k+1)$.

	ord Gdh	ord $\frac{1}{G}dh$	$\angle Gdh$	$\angle\frac{1}{G}dh$	$\angle dh$
H_1	0	2	$\pi/2$	$3\pi/2$	π
H_2	2	0	$3\pi/2$	$\pi/2$	π
H_3	0	2	$\pi/2$	$3\pi/2$	π
H_4	2	0	$3\pi/2$	$\pi/2$	π
H_5	0	2	$\pi/2$	$3\pi/2$	π
H_6	2	0	$3\pi/2$	$\pi/2$	π
H_7	0	2	$\pi/2$	$3\pi/2$	π
H_8	2	0	$3\pi/2$	$\pi/2$	π
H_9	0	2	$\pi/2$	$3\pi/2$	π
E	-2	-4	$-\pi/2$	$-3\pi/2$	$-\pi$

Figure 8: Divisors and Cone angles for the forms Gdh and $\frac{1}{G}dh$

Here the last three columns give one-fourth of the total cone angle at the indicated point: we display just one-fourth of the angle as the one-fourth of the surface we display includes just one-fourth of a neighborhood of each of these points.

In every one of the situations we treat, we may assume that the surface is sufficiently symmetric so as to guarantee that a fundamental domain is planar. Indeed, a drawback of our method is that it is not immediately clear how to extend this method to the case wher the fundamental domain of the minimal surface is non-planar surface, or even a topologically non-trivial planar surface. So, we focus for the rest of the time on topological disks with flat structures.

Definition 3.1.1. *An orthodisk is a closed topological disk, with distinguished points on the boundary, equipped with a both a Euclidean metric and with an isometric developing into* $\mathbb{E}^2$*. The Euclidean metric renders the intervals between the distinguished points as non-singular geodesics; we label these intervals by their endpoints.*

We typically blur the distinction between the orthodisk and its developed image in $\mathbb{E}^2$.

We are almost in a position from which we can display the possible flat structures for the forms Gdh, $\frac{1}{G}dh$ and dh; we will of course now refer to these structures as the orthodisks for Gdh, $\frac{1}{G}dh$ and dh. Before doing that however, we note that in this particular situation, we find one more restriction from our simulation which is particularily helpful: we see a straight line on the surface connecting the middle handle point H_5 with the end E. We will thus require all of our forms to respect the symmetry across this line. With this in mind, we claim that the developed image of the form Gdh looks like the domain to the upper left in the figure below.

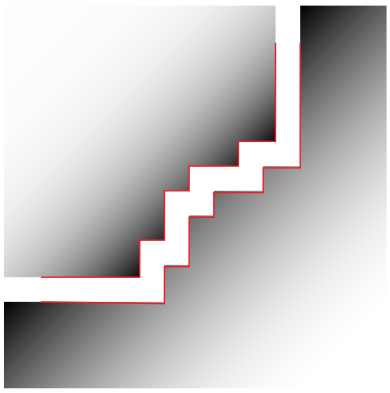

Figure 9: Flat structures for Gdh for E_4

Here we should imagine that when we label the vertices counter-clockwise: the first finite vertex is H_1, the final finite vertex is H_9, and the end E is at infinity. We see from the table just above that the angles at the H_i are correct, and it is not much harder to decide that the angle at the infinite end E is also correctly represented. We have also imposed the symmetry about the line on the surface from H_5 to E by requiring a reflective symmetry about the diagonal line in the diagram from H_5 to E.

Finally, we remark that the process of deriving a domain, say Ω_{Gdh}, from a Riemann surface and the one-form Gdh, is reversible. One begins with such a domain, and then takes a branched double cover (branched over the vertices) over the double of the domain. The one-form dz pulls back to give the desired form: Gdh in this case.

3.2 Representing the Period Problem

We now take up the problem of representing periods in these flat structures. The basic observation is that if we develop via a formula like

$$z(\zeta) = \int^{\zeta} Gdh \tag{3.2.1}$$

to obtain a domain, say Ω_{Gdh} in the z-plane as in Figure 9, then the Fundamental Theorem of Calculus implies that we may represent the form Gdh in that domain Ω_{Gdh} as dz. But then, for an arc γ on the surface that develops into the plane as $z(\gamma)$, we find that

$$\int_{\gamma} Gdh = \int_{z(\gamma)} dz \tag{3.2.2}$$

and this last integral is simply the difference of the z-values of the endpoints of $z(\gamma)$.

With this in mind, we observe from the topology of the simulation in Figure 6 that any cycle on the minimal surface E_4 projects to be homologous to a sum of edges in the boundary $\partial\Omega_{Gdh}$. Thus, since from the previous paragraph we have on Ω_{Gdh} the representation of $Gdh = dz$, we see that the periods of Gdh are expressible as sums of the (complex) lengths of the sides (i.e the difference of the endpoints of the segments as complex numbers).

Thus, the period condition, expressed analytically as

$$\int_\gamma Gdh = \overline{\int_\gamma \frac{1}{G} dh} \tag{3.2.3}$$

translates to a geometric condition that the complex length of an edge H_iH_{i+1} in Ω_{Gdh} should be the conjugate of the complex length of the corresponding edge H_iH_{i+1} in $\Omega_{\frac{1}{G}dh}$.

This brings us to an idiosyncrasy of our construction. We find it easier to construe our vertical planes as being vertical coordinate planes so that Ω_{Gdh} has horizontal and vertical boundary edges. Also, then the analogous domain $\Omega_{\frac{1}{G}dh}$ will also have horizontal and vertical boundary edges. But, in order to force (3.2.3), we will then have to construe the real line in the figure Figure 9 as being diagonal, parallel to the line $\{y = x\}$.

From these considerations, we can use the domain Ω_{Gdh} and the table of cone angles of Figure 3.1 above to force a precise description of the domain $\Omega_{\frac{1}{G}dh}$. Indeed, this is the domain in Figure 9 which is complementary to Ω_{Gdh}; here since we keep the domain to the left of the boundary, we label the points in an manner *opposite* to how we labelled them for Ω_{Gdh}, i.e. the first finite point H_1 is the corner at the top right, while the last finite point, H_9 is the corner at the bottom left.

Definition 3.2.1. *A pair of similarly labelled orthodisks Ω_1 and Ω_2 are called conjugate if, after lifting the canonical form dz from $\mathbb{E}^2$ to the surfaces S_1 and S_2 which (branched) doubly covers Ω_1 and Ω_2, respectively, the periods of the forms are conjugate.*

We observe that this condition can be verified by considering arcs which connect corresponding boundary edges of Ω_1 and Ω_2, as long as we keep in mind that these arcs are only one piece of an entire circle on the surfaces S_i.

It is now evident why the symmetry we imposed about the diagonal line from H_5 to E is so useful: because of that symmetry, the segments $\overline{H_iH_{i+1}}$ and $\overline{H_{9-i}H_{10-i}}$ have the same length and opposite orientation in both domains Ω_{Gdh} and $\Omega_{\frac{1}{G}dh}$, and these oreintations are reversed for the 'complementary' domain. The upshot is that these two orthodisks, Ω_{Gdh} and $\Omega_{\frac{1}{G}dh}$, when drawn as in Figure 9 precisely fit together so that the closure of their union is exactly $\mathbb{C}$.

Where has the (horizontal) period problem (3.2.3) gone? We really haven't done anything – developing one-forms into $\mathbb{C}$ cannot be anything beyond a psychological convenience – but we have displayed domains where (3.2.3) is satisfied. However, when we drafted these domains using the condition (3.2.3), we ignored the conformal structure of the resulting domains. What we have accomplished in this process of describing a pair of conjugate orthodisks Ω_{Gdh} and $\Omega_{\frac{1}{G}dh}$ is the transformation of the period problem into a:

Conformal Problem: Find two such conjugate domains Ω_{Gdh} and $\Omega_{\frac{1}{G}dh}$ which are conformal by a map which takes vertices H_i and E to corresponding vertices H_i and E.

Solving this problem then solves the (horizontal) period problem, as we can begin with the conformal structure common to both Ω_{Gdh} and $\Omega_{\frac{1}{G}dh}$, and then take the branched cover of the double of either domain to obtain a Riemann surface. Then the canonical one-forms dz on each domain lift to forms Gdh and $\frac{1}{G}dh$ on that Riemann surface which, by construction, satisfy (3.2.3).

Remark 3.2.2. *We can also follow this process to produce a orthodisk, say Ω_{dh} corresponding to the one-form dh. A surprising feature of the proofs of all the theorems in the introduction is that finding a domain Ω_{dh} appropriately conformal to Ω_{Gdh} and $\Omega_{\frac{1}{G}dh}$ which satisfies the period condition* $\mathrm{Re}\int_\gamma dh = 0$

is automatic. In particular, in the case of the Enneper-ended surfaces E_g, this reflects that such forms dh are exact.

A more thorough discussion of orthodisks and Weierstraß data can be found in [WW].

3.2.1 Orthodisks for other minimal surfaces

We pause for a moment from our treatment of the orthodisks relevant to the Enneper-ended surfaces E_g to display the geometries of orthodisks relevant for the study of other surfaces.

We begin by noting that when we compute the orthodisks for the "higher genus" Costa surfaces CT_g, we get surfaces with more sheets and more branch points, as in the Figures 10 and 11. (Here branch points are indicated by fat dots.)

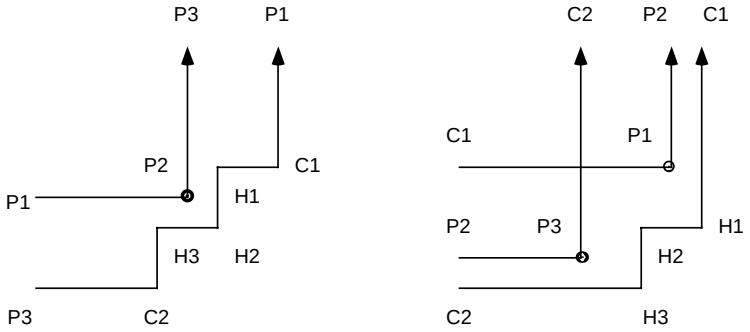

Figure 10: orthodisks for a genus three Costa surface

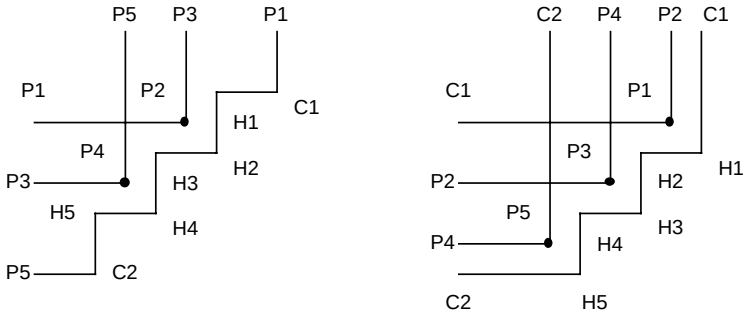

Figure 11: orthodisks for a genus five Costa surface

The doubly periodic Scherk surfaces with handles (as in Figure 12) have orthodisks like those pictured in Figure 13.

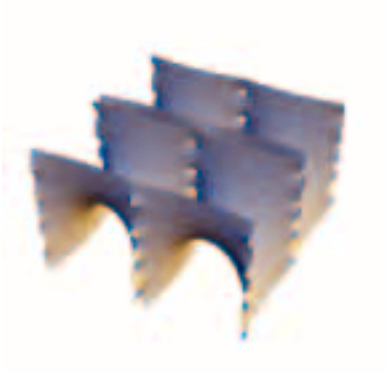

Figure 12: the genus 4 doubly periodic Scherk

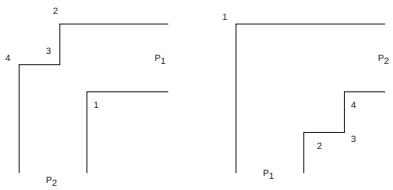

Figure 13: orthodisks for genus 4 doubly periodic Scherk

3.3 Moduli spaces of Conjugate Flat Structures

How are we to solve the conformal problem of the last subsection? The basic approach is to regard that problem as a problem in the moduli spaces of pairs of conjugate orthodisks Ω_{Gdh} and $\Omega_{\frac{1}{G}dh}$. In particular, observe that the domain Ω_{Gdh}, because of the symmetry about the line H_5E is determined by the edge lengths of the segments $\overline{H_iH_{i+1}}$ for $i = 1, 2, 3, 4$. The conformal structure (here we *always* mean by "conformal structure" that the points H_i and E are distinguished) is also given by these numbers, up to scaling. Thus the moduli space $\mathcal{M}_4$ of possible conformal structures of domains Ω_{Gdh} for the surface E_4 is given as the simplex $\mathcal{M}_4 = \{(x_1, x_2, x_3, x_4) | \sum x_i = 1, x_i > 0\}$. As such domains immediately define $\Omega_{\frac{1}{G}dh}$ by construction (in this case, by taking the complementary domain in $\mathbb{C}$), we see that solving the conformal problem in $\mathcal{M}_4$ is equivalent to producing the minimal surface E_4.

Before outlining how we solve that conformal problem, we pause briefly to explore these moduli spaces.

3.3.1 A singleton moduli space: The Costa surface $DH_{0,0}$ $(= CT_0)$

The Costa surface is the basic example of a complete finite total curvature embedded minimal surface of non-trivial topology. It is also the starting point for the investigations for the Theorem 1.0.3. Here, we seek a torus with two catenoid ends (C_1 and C_2), one planar end P_1 and one finite point H_1 with vertical normal. We also assume our standard eight symmetries: reflections about two orthogonal vertical planes and a rotation about a horizontal line. (Previous existence and uniqueness proofs may be found in [Cos84] and [HMI85])

As we did for the surface E_4 in subsection 3.1, we can deduce the divisor data for the Weierstraß data for this surface, assuming that the points occur on the boundary of a fundamental quarter of the surface in the order $C_1 - P_1 - C_2 - H_1$. (Below we reproduce a computer image of a fundamental domain of Costa's surface for the group generated by reflections in the two vertical planes. This makes apparent the conformal polygon, and the order of the special points on its boundary.)

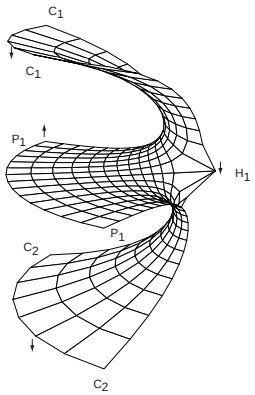

Figure 14: One Quarter of Costa's surface

A table corresponding to 3.1 is given below; it computes the cone angles for the forms Gdh and $G^{-1}dh$ on the putative conformal polygon for Costa's surface. These flat structures are drawn below, assuming again an additional symmetry about the line $\{y = -x\}$.

	ord G	ord dh	ord Gdh	ord $\frac{1}{G}dh$	$\angle Gdh$	$\angle \frac{1}{G}dh$	$\angle dh$
$C_1 \downarrow$	1	-1	0	-2	$\pi/2$	$-\pi/2$	0
$P_1 \uparrow$	-3	1	-2	4	$-\pi/2$	$5\pi/2$	π
$C_2 \downarrow$	1	-1	0	-2	$\pi/2$	$-\pi/2$	0
$H_1 \downarrow$	1	1	2	0	$3\pi/2$	$\pi/2$	π

Figure 15: Divisors and (quarter) cone angles for Costa's surface

The crucial observation to make at this point is that any conformal quadrilateral with a symmetry across a diagonal is conformally equivalent to a square.

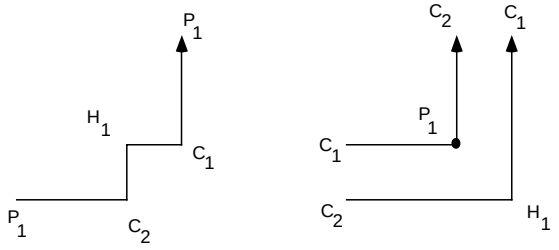

Figure 16: orthodisks for Gdh and $\frac{1}{G}dh$ for Costa's surface

Thus we conclude that the moduli space of possible examples consists only of the singleton of a pair of square tori, so the only element in the moduli space is a reflexive pair. This establishes the existence of this surface, by a proof that is somewhat distinct from the other proofs of existence of this surface ([Cos84], [HK97]).

3.3.2 Empty moduli spaces: Catenoid with one handle

In this example, we try to construct a minimal surface with two catenoid ends and one handle; in addition, here we will also require the eightfold symmetry present in all of our examples. Now, a well-known theorem

of Schoen [Sch83] implies that any minimal surface of genus $g \geq 1$ with but two embedded catenoid ends cannot exist; still this particular example provides for a simple introduction to our style of argument for non-existence, so this problem is worth addressing from the orthodisk perspective. Now, it is clear from an analysis of the orthodisks pictured below that such a surface cannot exist with 4-fold symmetry, because there is no symmetric and conjugate pair: the periods from $\overline{C_1C_2}$ to $\overline{H_1H_2}$ are conjugate about the line $\{y = -x\}$, while the periods from $\overline{C_2H_2}$ to $\overline{H_1C_1}$ are conjugate across the line $\{y = +x\}$.

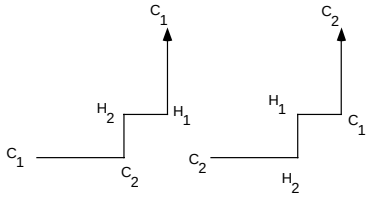

Figure 17: Catenoid with a handle

A crucial part of Theorem 1.0.4 is the proof of the non-existence of a whole class of possible configurations, consistent with the Hoffman-Meeks conjecture. The technique we use there is mostly just an iterative use of the technique we exhibit here for the non-existence of the one-handled catenoid.

3.3.3 The Horgan surface $DH_{0,1}$

The second example of non-existence is called the Horgan surface (see [HK97]): to visualize it, start with one plane and two handles, one growing upwards and another growing downwards – the necks of the handles should be perpendicular to one another. Both handles connect to catenoid ends. One imagines the surface to look almost as pictured in the following figure:

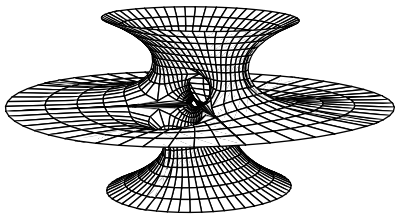

Figure 18: The Horgan surface??

This pattern leads to a sequence of distinguished points on the boundary in the order

$$C_1 - P - C_2 - H_2 - M - H_1 - C_1$$

where M denotes a (new type of) regular point where the symmetry lines cross. The orthodisks are as follows:

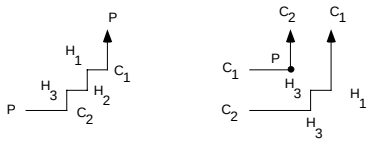

Figure 19: orthodisks corresponding to the Horgan surface

Recently, Weber [Web98] showed that this surface cannot exist by a method that is different from that used in our previous non-existence proofs. Here there is a non-trivial moduli space, but our general existence proof fails at precisely one place for the case of this class of surface (we are unable to prove "Properness of the Height Function").

4 Architecture of the Proof

4.1 Converting the Period Problem into a Conformal Problem

Our goal in this section is to outline the approach we use to prove the theorems stated at the outset of this note.

While the details of the arguments are sometimes quite involved, the basic logic of the approach and the ideas of the proofs are quite simple. Here, we outline the argument, as a step-by-step recipe. (For the sake of making this section somewhat self-contained, we repeat some of the background we developed in computing the orthodisks for E_4.)

Step 1. Draw the Surface. The first step in proving the existence of a minimal surface is to work out a detailed proposal. This can either be done numerically, as in the work of Thayer [Tha94] for the Chen-Gackstatter surfaces E_g or in Boix and Wohlgemuth ([BW]) for the low genus surfaces of the classes CT_g – or it can be schematic, showing how various portions of the surface might fit together. Often, as in the case of E_4 above we need to narrow the list of possibilities, and so additional symmetries might be assumed. Sometimes, there are quite a few combinatorial possibilities, and so, for each such class, we might attempt to follow the recipe and see if any of the rest of recipe fails.

Step 2. Compute the Divisors for the Forms Gdh and $\frac{1}{G}dh$. From the model that we drew in Step 1, we can compute the divisors for the Weierstraß data, which we earlier defined to be the Gauss map G and the 'height' form dh. (Note here how important it is that the Weierstraß representation be given in terms of geometrically defined quantities – for us, this gives the passage between the extrinsic geometry of the minimal surface as defined in Step 1 and the conformal geometry and Teichmüller theory of the later steps.) Thus we can also compute the divisors for the meromorphic forms Gdh and $\frac{1}{G}dh$ on the Riemann surface (so far undetermined, but assumed to exist) underlying the minimal surface. Of course the divisors for a meromorphic form (on a compact surface) determine the form up to a constant, so the divisor information nearly determines the Weierstraß data for our surface. For the surface E_4, this step was completed in the Table 3.1.

Step 3. Compute the Orthodisks for the Forms Gdh and $\frac{1}{G}dh$ required by the period conditions. A meromorphic form on a Riemann surface defines a flat singular (conformal) metric on that surface: for example, from the form Gdh on our putative Riemann surface, we determine a line element $ds_{Gdh} = |Gdh|$. This metric is locally Euclidean away from the support of the divisor of the form and has a complete Euclidean cone structure in a neighborhood of a zero or pole of the form. Thus we can develop the universal cover of the surface into the Euclidean plane.

The orthodisks for the forms Gdh and $\frac{1}{G}dh$ are not completely arbitrary: because the periods for the pair of forms must be conjugate by formula (3.2.3), the orthodisks must develop into domains which have a particular Euclidean geometric relationship to one another. This relationship is crucial to our approach, so we will dwell on it somewhat (generalizing the discussion of section 3.2). If the map $D : \Omega \longrightarrow \mathbb{E}^2$ is the map which develops the flat structure of a form, say α, on a domain Ω into $\mathbb{E}^2$, then the map D pulls

back the canonical form dz on $\mathbb{C} \cong \mathbb{E}^2$ to the form α on Ω. Thus the periods of α on the Riemann surface are given by integrals of dz along the developed image of paths in $\mathbb{C}$, i.e. by differences of the complex numbers representing endpoints of those paths in $\mathbb{C}$.

We construe all of this as requiring that the flat structures develop into domains that are "conjugate": if we collect all of the differences in positions of parallel sides for the developed image of the form Gdh into a large complex-valued n-tuple V_{Gdh}, and we collect all of the differences in positions of corresponding parallel sides for the developed image of the form $\frac{1}{G}dh$ into a large complex-valued n-tuple $V_{\frac{1}{G}dh}$, then these two complex-valued vectors V_{Gdh} and $V_{\frac{1}{G}dh}$ should be conjugate. This is the flat structure implication of the period condition formula (3.2.3), here using that our situation allows that the periods of all cycles can be found from differences of positions of parallel sides in a flat structure. Thus, we translate the "period problem" into a statement about the Euclidean geometry of the developed flat structures. This we already did for the surface E_4 in section 3.

As we remarked earlier, the vertical period problem ($\mathrm{Re}\int_\gamma dh = 0$) will be trivially solved for the surfaces we treat here.

Step 4. Define the moduli space of pairs of conjugate flat domains. Now we work backwards. We know the general form of the developed images (called Ω_{Gdh} and $\Omega_{\frac{1}{G}dh}$, respectively) of orthodisks associated to the forms Gdh and $\frac{1}{G}dh$, but in general, there are quite a few parameters of the orthodisks left undetermined, even after we have assumed symmetries, determined the Weierstraß divisor data for the models and used the period conditions (3.2.3) to restrict the relative Euclidean geometries of the pair Ω_{Gdh} and $\Omega_{\frac{1}{G}dh}$. Thus, there is a moduli space Δ of possible candidates of pairs Ω_{Gdh} and $\Omega_{\frac{1}{G}dh}$: our period problem (3.2.3) is now a conformal problem of finding such a pair which are conformally equivalent by a map which preserves the corresponding cone points. (Solving this problem means that there is a well-defined Riemann surface which can be developed into $\mathbb{E}^2$ in two ways, so that the pair of pullbacks of the form dz give a pair of forms Gdh and $\frac{1}{G}dh$ with conjugate periods.)

[The condition of conjugacy of the domains Ω_{Gdh} and $\Omega_{\frac{1}{G}dh}$ often dictates some restrictions on the moduli space, and even a collection of geometrically defined coordinates. We do not meet these in the considerations of the surface E_g, but they are crucially relevant in the discussion of the surfaces CT_g, where they enter into the proof of non-existence of some candidates. We saw a brief glimmer of this in our discussion of the non-existence of the catenoid with a handle.]

Step 5. Solve the Conformal Problem using Teichmüller theory. At this juncture, our minimal surface problem has become a problem in finding a special point in a product Δ of moduli spaces of complex domains: we will have no further references to minimal surface theory. The plan is straightforward: we will define a height function $\mathcal{H} : \Delta \longrightarrow \mathbb{R}$ with the properties:

1. (Reflexivity) The height $\mathcal{H}$ equals 0 only at a solution to the conformal problem.
2. (Properness) The height $\mathcal{H}$ is proper on Δ. This ensures the existence of a critical point.
3. (Non-Critical Flow) If the height $\mathcal{H}$ at a pair $(\Omega_{Gdh}, \Omega_{\frac{1}{G}dh})$ does not vanish, then the height $\mathcal{H}$ is not critical at that pair $(\Omega_{Gdh}, \Omega_{\frac{1}{G}dh})$.

The proof of the solution to the conformal problem then summarizes as follows: we restrict to a locus $\mathcal{Y}$ on which we have the Non-Critical Flow Property. By Properness, the height function $\mathcal{H}$ is proper on $\mathcal{Y}$; thus there is a critical point X on $\mathcal{Y}$ for $\mathcal{H}$. The Non-Critical Flow then forces $\mathcal{H}(X) = 0$, so by Reflexivity, the surface represented by X is a solution to our conformal problem, and hence also defines a solution to the minimal surface problem.

We will see that Reflexivity will be relatively straightforward, but Properness and Non-Critical Flow will require some care. This is because in these latter two steps, we are forced to compare two flat structures of a domain (and their underlying conformal structures.) In the customary treatment of the period problem, the difficulty was in understanding periods of two one-forms on a single surface – here the periods of the one-forms have been transmuted into a flat structure on the Riemann surface, and so the basic difficulty of the original global problem emerges in relating the pair of orthodisks.

How should we define this height function? We need a finite number of conformal invariants of Ω_{Gdh} and $\Omega_{\frac{1}{G}dh}$ which

1. (Reflexivity) form a complete set of conformal invariants, i.e. the two domains Ω_{Gdh} and $\Omega_{\frac{1}{G}dh}$ are conformally equivalent if and only if the given set of conformal invariants agree,
2. (Properness) have computable/estimable asymptotics, and
3. (Non-Critical Flow) have computable derivatives.

The natural candidates for these invariants are the "Extremal Lengths" of curve systems, first defined by Beurling and Ahlfors in the 1940's. (We discuss the rudiments of this subject below: see [Ahl66] or [Oht70] for more details.)

Before plunging into a discussion of extremal lengths, we provide a context by just producing a height function for the Enneper-ended surfaces E_g. In this discussion, the curves Γ_i refer to the set of arcs in the domain which have one endpoint on $H_{i-1}H_i$ and another endpoint on $H_{i+1}H_{i+2}$ (where here we construe $H_0 = E$).

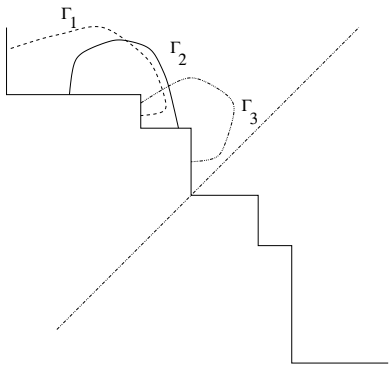

Figure 20: Curve systems for E_4

Remark 4.1.1. *In general, the decision about which curve systems to use is the one aspect of the proof which is not yet automatic – presently, we do not have a good procedure for deciding from a pair of orthodisks how to choose a system of curves for the height function which will allow for all three aspects of the proof to work at once.*

We define the height as

$$\mathcal{H} = \sum_{i=1}^{n} \mathcal{H}(\Gamma_i) \tag{4.1.1}$$

with

$$\mathcal{H}(\Gamma_i) = \left(\mathrm{Ext}_{\Gamma_i}(\Omega_{Gdh}) - \mathrm{Ext}_{\Gamma_i}(\Omega_{\frac{1}{G}dh})\right)^2 + \left(e^{\frac{1}{\mathrm{Ext}_{\Gamma_i}(\Omega_{Gdh})}} - e^{\frac{1}{\mathrm{Ext}_{\Gamma_i}(\Omega_{\frac{1}{G}dh})}}\right)^2 \tag{4.1.2}$$

[Here, the idea is to compare corresponding extremal lengths on Ω_{Gdh} and $\Omega_{\frac{1}{G}dh}$. We discuss the form of each term when we discuss Properness.]

4.2 Background on Extremal Length

Before resuming our outline, we pause to recall some aspects of the notion of Extremal Length. The definition of Extremal Length is very very flexible. Consider a *set* Γ of curves on a Riemann surface $\mathcal{R}$, and

the set $\mathcal{M} = \{\rho \geq 0\}$ of (measurable) conformal metrics on that Riemann surface. We define the Extremal Length of Γ on $\mathcal{R}$ to be

$$Ext_{\mathcal{R}}(\Gamma) = \sup_{\rho \in \mathcal{M}} \frac{\inf_{\gamma \in \Gamma} [\ell_\rho(\gamma)]^2}{area_\rho(\mathcal{R})} \tag{4.2.1}$$

Here, $\ell_\rho(\gamma)$ is the ρ-length of γ and $area_\rho$ is the ρ-area of the Riemann surface $\mathcal{R}$.

The idea is that this gives some notion of length that depends only on the underlying Riemann surface $\mathcal{R}$, and not on a choice of conformal metric on $\mathcal{R}$.

Here are three useful observations that guide many of our choices – we will not refer to it explicitly in the sequel, but it is crucial for some of the details of the arguments that we are omitting in this treatment. First, as $Ext_{\mathcal{R}}(\Gamma)$ is a supremum, we immediately obtain a lower bound for this invariant of extremal length from any conformal metric in which we can estimate shortest lengths.

On the other hand, since Γ is usually taken to be a homotopy class of simple curves, we can characterize the solution metric and thus obtain a different definition of Extremal length. In particular, an easy length-area argument (see [Ahl66]) shows that the solution metric for the curves in a $h \times l$ rectangle connecting opposite sides is given by the standard flat metric on that rectangle.

We can thus equivalently define

$$Ext_{\mathcal{R}}(\Gamma) = \inf_{R_{h \times \ell} \subset \mathcal{R}} \frac{\ell}{h} \tag{4.2.2}$$

where the infimum is over all $h \times l$ rectangles $R_{h \times l}$ embedded in $\mathcal{R}$ with horizontal curves in Γ.

This new definition, now in terms of an infimum, allows us to obtain *upper* bounds for $Ext_{\mathcal{R}}(\Gamma)$ by mapping in appropriate rectangles (or annuli if the curves in Γ are closed).

Finally, as we can explicitly solve the extremal length problems for points on curves encircling boundary points of a disk, we know estimates for how extremal length changes with infinitesimal changes of data, as well as under degeneration. Also, the formulae are invertible: given the extremal lengths of $n-3$ cycles encircling consecutive pairs of points, we can locate the n points.

This last fact allows us to conclude that for these pairs, say Z, of planar domains, we have $\mathcal{H}(Z) = 0$ if and only if Z represents a conformal pair of conjugate domains.

4.3 Analysis of the Height Function

We now return to our outline of the proof of the theorem.

4.3.1 Step 5a. Reflexivity.

Having defined the height function via the extremal lengths of the curves Γ_i, for a good choice of Γ_i, this step of refelxivity is always immediate, at least for the case of a pair of domains Ω_{Gdh} and $\Omega_{\frac{1}{G}dh}$ which are topological disks. (It is at present far from clear how to extend this architecture to the case of topologically non-trivial orthodisks.) We simply recall from the previous subsection that to determine the position of n boundary points of a disk, we require the extremal lengths of $n-3$ distinct arcs encircling pairs of those boundary points. Our height function is constructed so that it vanishes only when such a set of extremal lengths for both domains agree.

4.3.2 Step 5b Properness.

We need to show that as one of the conformal structures, (underlying one of the orthodisks Ω_{Gdh} or $\Omega_{\frac{1}{G}dh}$) degenerates, then the height of the pair goes to infinity. The subtlety here is that the asymptotic differences in the extremal lengths of corresponding surfaces can be quite minute: our height function is specifically created to blow up these small differences.

Our height function will measure differences in the extremal lengths $Ext_{\Omega_{Gdh}}(\gamma_i)$ and $Ext_{\Omega_{\frac{1}{G}dh}}(\gamma_i)$. Often, but not always, a geometric degeneration of the orthodisk of either Ω_{Gdh} or $\Omega_{\frac{1}{G}dh}$ will force one

of the extremal lengths $Ext_\bullet(\gamma_i)$ to tend to zero or infinity, while the other extremal length stays finite and bounded away from zero. This is a straightforward situation where it will be obvious that the height function will blow up. A more subtle case arises when a geometric degeneration of the orthodisk forces *both* of the extremal lengths $Ext_{\Omega_{G\,dh}}(\gamma_i)$ and $Ext_{\Omega_{\frac{1}{G}\,dh}}(\gamma_i)$ to *simultaneously* decay (or explode). In that case, we begin by observing that there is a natural map between the vector $< Ext_{\Omega_{G\,dh}}(\gamma_i) >$ and the vector $< Ext_{\Omega_{\frac{1}{G}\,dh}}(\gamma_i) >$. This pair of vectors is reminiscent of pairs of solutions to a hypergeometric differential equation, and we show, by a monodromy argument analogous to that used in the study of those equations, that it is not possible for corresponding components of that vector to vanish or blow up at identical rates. In particular, we show that the logarithmic terms in the asymptotic expansion of the extremal lengths near zero have a different sign, and this sign difference forces a difference in the rates of decay that is detected by the height function, forcing it to blow up in this case. In the next paragraph, we give some of the crucial details of this monodromy argument.

The Monodromy Argument. Let Δ be a moduli space of dimension at least 2 parametrizing pairs of orthodisks X_1 and X_2 corresponding to given formal Weierstraß data as usual. Suppose γ is a cycle in the underlying conformal polygon which joins edges P_1P_2 and Q_1Q_2 which are parallel (and hence non-adjacent) in the flat structures. (In our applications, γ will be one of the cycles used in the height function). Denote by R_1 the vertex before Q_1 and by R_2 the vertex after Q_2 and observe that by assumption, $R_2 \neq P_1$ and $P_2 \neq R_1$. Introduce a second cycle β which connects R_1Q_1 with Q_2R_2.

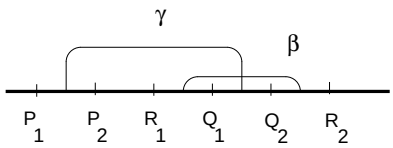

Figure 21: Local Picture for Monodromy Argument

We formulate our properness claim more precisely in the following two lemmas:

Lemma 4.3.1. *Suppose that for a sequence $p_n \in \Delta$ with $p_n \to p_0 \in \partial\Delta$ we have that* $\mathrm{Ext}_{X_1(p_n)}(\gamma) \to 0$ *and* $\mathrm{Ext}_{X_2(p_n)}(\gamma) \to 0$. *Suppose furthermore that γ is a cycle encircling a single edge which degenerates geometrically to 0 as $n \to \infty$ in $X_1(p_n)$. Then*

$$|e^{1/\,\mathrm{Ext}_{X_1(p_n)}(\gamma)} - e^{1/\,\mathrm{Ext}_{X_2(p_n)}(\gamma)}|^2 \to \infty$$

Lemma 4.3.2. *Suppose that for a sequence $p_n \in \Delta$ with $p_n \to p_0 \in \partial\Delta$ we have that* $\mathrm{Ext}_{X_1(p_n)}(\gamma) \to \infty$ *and* $\mathrm{Ext}_{X_2(p_n)}(\gamma) \to \infty$. *Suppose furthermore that γ is a cycle with an endpoint on an edge which degenerates geometrically to 0 as $n \to \infty$ in $X_1(p_n)$. Then*

$$|e^{\mathrm{Ext}_{X_1(p_n)}(\gamma)} - e^{\mathrm{Ext}_{X_2(p_n)}(\gamma)}|^2 \to \infty$$

Proof. We first prove Lemma 4.3.1, assuming for now a later Corollary 4.3.3.

Corollary 4.3.3. *Either $\|F_1(\gamma)\| - \frac{\log\delta}{\pi}\|F_1(\beta)\|$ or $\|F_1(\gamma)\| + \frac{\log\delta}{\pi}\|F_1(\beta)\|$ is real analytic in δ for $\delta = 0$. In the first case, $\|F_2(\gamma)\| + \frac{\log\delta}{\pi}\|F_2(\beta)\|$ is real analytic in δ, in the second $\|F_2(\gamma)\| - \frac{\log\delta}{\pi}\|F_1(\beta)\|$.*

Consider the conformal polygons corresponding to the pair of orthodisks. Normalize the punctures by Möbius transformations so that

$$P_1 = -\infty, P_2 = 0, Q_1 = \epsilon, Q_2 = 1 \tag{4.3.1}$$

for X_1 and

$$P_1 = -\infty, P_2 = 0, Q_1 = \epsilon', Q_2 = 1 \tag{4.3.2}$$

for X_2. By the assumption of Lemma 4.3.1, we know that $\epsilon, \epsilon' \to 0$ as $n \to \infty$. We now apply the monodromy Corollary 4.3.3 above to the curve $\epsilon_0 e^{it}$ and conclude that either

$$\frac{|\operatorname{Per}\beta(X_1)|}{|\operatorname{Per}\gamma(X_1)|} + \frac{1}{\pi}\log\epsilon \tag{4.3.3}$$

is single-valued in ϵ while

$$\frac{|\operatorname{Per}\beta(X_2)|}{|\operatorname{Per}\gamma(X_2)|} - \frac{1}{\pi}\log\epsilon' \tag{4.3.4}$$

is single-valued in ϵ', or the same statement holds for the analogous quantities with opposite signs. Without loss of generality, we can treat the first case.

Now suppose that ϵ' is real analytic (and hence single-valued) in ϵ near $\epsilon = 0$. Then using that X_1 and X_2 are conjugate implies that the absolute lengths of β in X_1 and X_2 are equal, as are those of γ; hence

$$\frac{|\operatorname{Per}\beta(X_1)|}{|\operatorname{Per}\gamma(X_1)|} = \frac{|\operatorname{Per}\beta(X_2)|}{|\operatorname{Per}\gamma(X_2)|}. \tag{4.3.5}$$

Thus we see, after subtracting 4.3.4 from 4.3.3, that

$$\log(\epsilon\epsilon'(\epsilon)) \tag{4.3.6}$$

is single-valued in ϵ near $\epsilon = 0$ which contradicts that $\epsilon, \epsilon' \to 0$.

Now Ohtsuka's [Oht70] extremal length formula states that for the current normalization of $X_1(p_n)$ we have

$$\operatorname{Ext}(\gamma) = O\left(|\log\epsilon|^{-1}\right) \tag{4.3.7}$$

(see Lemma 4.5.3 in [WW98] and [Oht70]). We conclude that

$$|e^{1/\operatorname{Ext}_{X_1(p_n)}(\gamma)} - e^{1/\operatorname{Ext}_{X_2(p_n)}(\gamma)}| = O\left(\frac{1}{\epsilon} - \frac{1}{\epsilon'}\right) \tag{4.3.8}$$

which goes to infinity, since we have shown that ϵ and ϵ' tend to zero at different rates. This proves Lemma 4.3.1.

The proof of Lemma 4.3.2 is very similar: for convenience, we normalize the points of the punctured disks such that

$$P_1 = -\infty, P_2 = 0, Q_1 = 1, Q_2 = 1 + \epsilon \tag{4.3.9}$$

for X_1 and

$$P_1 = -\infty, P_2 = 0, Q_1 = 1, Q_2 = 1 + \epsilon' \tag{4.3.10}$$

for X_2.

By the assumption of Lemma 4.3.2, we know that $\epsilon, \epsilon' \to 0$ as $n \to \infty$. We now apply the monodromy Corollary 4.3.3 above to the curve $1 + \epsilon_0 e^{it}$ and conclude that

$$\frac{\operatorname{Per}\gamma(X_1)}{\operatorname{Per}\beta(X_1)} + \frac{1}{\pi}\log\epsilon \tag{4.3.11}$$

is single-valued in ϵ while

$$\frac{\operatorname{Per}\gamma(X_2)}{\operatorname{Per}\beta(X_2)} - \frac{1}{\pi}\log\epsilon' \tag{4.3.12}$$

is single-valued in ϵ'. The rest of the proof is identical to the proof of Lemma 4.3.1. □

To prove this important Corollary 4.3.3, we will need asymptotic expansions of the extremal length in terms of the Euclidean geometric invariants of the orthodisks. Though not much is known explicitly about extremal lengths in general, for the cycles we always choose we can reduce this problem to an asymptotic control of Schwarz-Christoffel integrals. Their monodromy properties allow us to distinguish their asymptotic behavior by the sign of logarithmic terms.

We introduce some notation: Suppose we have an orthodisk such that the angles at the vertices alternate between $\pi/2$ and $-\pi/2$ modulo 2π. Consider the Schwarz-Christoffel map

$$F : z \mapsto \int_i^z (t-t_1)^{a_1/2} \cdot \ldots \cdot (t-t_k)^{a_k/2} \tag{4.3.13}$$

from a conformal polygon with vertices at t_i to this orthodisk. Here we take each a_i to be an odd integer. Choose four distinct vertices $t_i, t_{i+1}, t_j, t_{j+1}$ so that $j \equiv i \pmod 2$, ensuring that the edges $t_i t_{i+1}$ and $t_j t_{j+1}$ are parallel in the orthodisk geometry. (See figure below.) Introduce a cycle γ in the upper half plane connecting edge (t_i, t_{i+1}) with edge (t_j, t_{j+1}) and denote by $\overline{\gamma}$ the closed cycle obtained from γ and its mirror image across the real axis. Similarly, denote by β the cycle connecting $(t_{j-1}t_j)$ with $(t_{j+1}t_{j+2})$ and by $\overline{\beta}$ the cycle together with its mirror image.

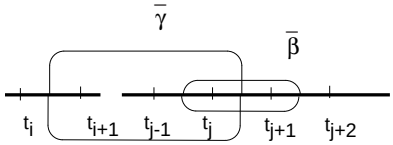

Figure 22: Cycles for analytic continuation

Now consider the Schwarz-Christoffel period integrals

$$\begin{aligned} F(\gamma) &= \frac{1}{2}\int_\gamma (t-t_1)^{a_1/2} \cdot \ldots \cdot (t-t_k)^{a_k/2} \\ F(\beta) &= \frac{1}{2}\int_\beta (t-t_1)^{a_1/2} \cdot \ldots \cdot (t-t_k)^{a_k/2} \end{aligned} \tag{4.3.14}$$

as multivalued functions depending on the *now complex* parameters t_i.

Theorem 4.3.4. *Under analytic continuation of t_{j+1} around t_j the periods change their values like*

$$\begin{aligned} F(\gamma) &\to F(\gamma) + 2F(\beta) \\ F(\beta) &\to F(\beta) \end{aligned} \tag{4.3.15}$$

To see this note that the path of analytic continuation of t_{j+1} around t_j gives rise to an isotopy of $\mathbb{C}$ which moves t_{j+1} along this path. This isotopy drags β and γ to new cycles we will call β' and γ', respectively.

Because the curve β is defined to surround t_j and t_{j+1}, the analytic continuation of t_j around t_{j+1} of merely returns β to β'. Thus, because β' equals β, their periods are also equal. On the other hand, the curve γ is not equal to the new 'dragged' curve γ'. To see this, note that the period of γ' is obtained by developing the flat structure of the doubled orthodisk along γ'. To compute this flat structure, observe the crucial fact that because the exponents in (4.3.13) are halves of odd integers, the angles at the orthodisk vertices are either $\pi/2$ or $-\pi/2$, modulo 2π; thus the angles of the doubled flat structure equal π, modulo 2π. Thus the arc γ' develops into the union of the arc γ *along with* the arcs β and $\overline{\beta}$; in particular, we see that the period of γ' equals the period of γ plus twice the period of β. □

Now denote by $\delta := t_{j+1} - t_j$ and fix all t_i other than t_{j+1}: we regard t_{j+1} as the independent variable.

Theorem 4.3.5. *The function $F(\gamma) - \frac{\log \delta}{\pi i} F(\beta)$ is single-valued and holomorphic near $\delta = 0$.*

Proof: By definition, the function is locally holomorphic near $\delta = 0$. By Theorem 4.3.4, it is single valued.

Now for the properness argument, we are interested in the geometric coordinates for the moduli space Δ – these are just the absolute values of the the periods. More precisely we are interested in

$$\|F(\gamma)\| := |\mathrm{Re}F(\gamma)| + |\mathrm{Im}F(\gamma)| \tag{4.3.16}$$

We translate the above statement about periods into a statement about their respective absolute values.

We consider two conjugate orthodisks parameterized by Schwarz-Christoffel maps F_1 and F_2 defined on the same conformal polygon. Recall that we have constructed β and γ to be either horizontal and vertical, respectively, or vertical and horizontal, respectively.

With this preparation, we can now prove the technical result Corollary 4.3.3 about degeneration that was the foundation for our properness argument.

Proof of Corollary 4.3.3: Recall that the above periods are linear combinations of the geometric coordinates where the coefficients are just elements of $\{1, -1, i, -i\}$. Now by construction, $F_j(\beta)$ is purely real or purely imaginary; moreover, the direction of $F_j(\beta)$ is $\pm i$ times the direction of $F_j(\gamma)$. This, together with Theorem 4.3.5, implies the first claim. Next, note that if we turn left at a vertex in the orthodisk X_1, we will turn right at the corresponding vertex in the conjugate orthodisk X_2, and vice versa. Thus, if the directions of the corresponding edges for γ in corresponding orthodisks differ by $+i$, then the directions of the corresponding edges for β will differ by a $-i$, and vice versa. This implies the second claim. □

This last Corollary 4.3.3 is really the crux of the properness argument: it is the critical ingredient in the proof of Lemma 4.3.1 and Lemma 4.3.2 that says that the extremal lengths of corresponding cycles on a pair of degenerating orthodisk domains cannot be real-analytically related. We have constructed the height function to exploit the precise differences in the orders of decay.

Remark 4.3.6. *Properness does require a pair of interlocking simple cycles as above. In very low genus, such pairs may not exist. This is exactly the (only) point at which a proof by our method fails to prove the existence of the Horgan surface.*

4.3.3 Steps 5c. and 5d., Non-Critical Flow and Regeneration.

We wish to show that if $Z_0 \in \Delta$ is a pair of conjugate orthodisks in the moduli space Δ, then if $\mathcal{H}(Z_0) \neq 0$, then we can embed Z_0 in a family $Z_t \subset \Delta$ so that $\frac{d}{dt}\mathcal{H}(Z_t) \neq 0$. There are two steps to this argument: first we observe that if we find ourselves on a one-dimensional locus $\mathcal{Y} = Z_t$ on which $Ext_{\Omega_{Gdh}}(\gamma_i) = Ext_{\Omega_{\frac{1}{G}dh}}(\gamma_i)$ for every γ_i with but one exception, then we can differentiate along that locus and find $\frac{d}{dt}\mathcal{H}(Z_t) \neq 0$. In the second step, we produce the locus $\mathcal{Y}$ by induction: this is the essence of the "handle addition" in the process. We begin in the next paragraph with the first step, and then conclude the Non-Critical Flow step with a discussion of the inductive "regeneration" in the following paragraph.

Non-Critical Flow along Good Loci The domains Ω_{Gdh} and $\Omega_{\frac{1}{G}dh}$ have a remarkable property: for many choices of cycles γ_i, if $Ext_{\Omega_{Gdh}}(\gamma_i) > Ext_{\Omega_{\frac{1}{G}dh}}(\gamma_i)$, then when we deform Ω_{Gdh} so as to decrease $Ext_{\Omega_{Gdh}}(\gamma_i)$, the conjugacy condition forces us to deform $\Omega_{\frac{1}{G}dh}$ so as to increase $Ext_{\Omega_{\frac{1}{G}dh}}(\gamma_i)$. We can thus always deform Ω_{Gdh} and $\Omega_{\frac{1}{G}dh}$ so as to reduce one term of the height function $\mathcal{H}$.

To see this, suppose that we are so lucky as to find ourselves at a Z where only the one "height" $\mathcal{H}(\Gamma_1) \neq 0$, i.e. we have equality of extremal lengths $Ext_{\Omega_{Gdh}}(\Gamma_i) = Ext_{\Omega_{\frac{1}{G}dh}}(\Gamma_i)$ of the "coordinate" cycles Γ_i for $i \neq 1$. As extremal length is given by conformally mapping the domain to a rectangle, we can imagine each half of an orthodisk being foliated by the image (under the conformal map) of the horizontal foliation of an appropriate rectangle. This is illustrated in the next Figure 23.

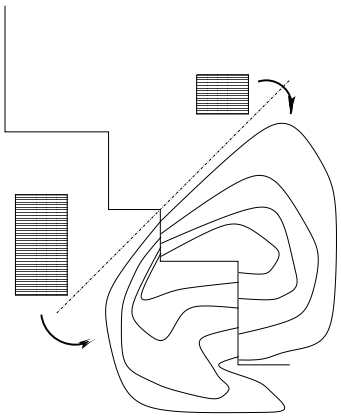

Figure 23: The image of the horizontal foliation of a rectangle foliates one of the halves of an orthodisk under a mapping by an appropriate conformal map. Typically, the rectangles required for Ω_{Gdh} and $\Omega_{\frac{1}{G}dh}$ will be conformally distinct.

Note that the foliations on Ω_{Gdh} and $\Omega_{\frac{1}{G}dh}$ extend to a (singular) foliation on $\mathbf{C}$. If $\mathrm{Ext}_{\Gamma_1}(\Omega_{Gdh}) > \mathrm{Ext}_{\Gamma_1}(\Omega_{\frac{1}{G}dh})$, we deform as follows, noting that we can simultaneously decrease $\mathrm{Ext}_{\Gamma_1}(\Omega_{Gdh})$ while increasing $\mathrm{Ext}_{\Gamma_1}(\Omega_{\frac{1}{G}dh})$.

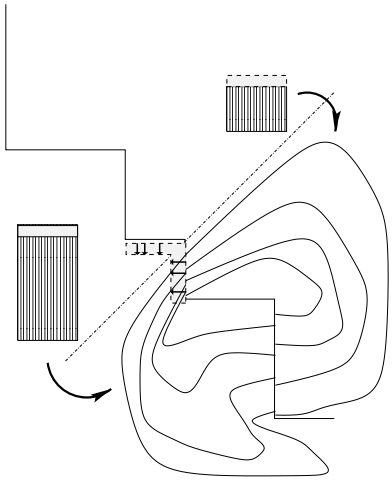

Figure 24: Heuristically, pushing a side decreases one extremal length while increasing the other. [See the bracketed remark below for a comment about how this heuristic is applied in the proof.]

(In fact, this situation only has to do with alternating left-right turns.) [Formally, we compute $\frac{d}{dt}\mathrm{Ext}_{\Gamma_1}(\Omega_{Gdh}(t))$, using well-known formulas [Gar87] about derivatives of extremal length functions on Teichmüller space and some of the elements of infinitesimal Teichmüller theory. In fact, when we do this carefully, we see that the heuristic above often does not quite work as drawn – typically we push on a side far away from the images of the corners of the rectangles.]

Remark 4.3.7. *Here we should point out that while this process seems quite robust, in very low genus (and in cases (see e.g. [WW] where the "good locus" $\mathcal{Y}$ is two-dimensional instead of one-dimensional), the proofs of this step become a bit more involved. See for example [WW].*

Regeneration. In the process described in the previous step, an issue arises: we might be able to reduce one term of the height function via a deformation, but this might affect the other terms, so as not to provide for an overall decrease in height. We thus seek a locus $\mathcal{Y}$ in our moduli space where the height function has but a single non-vanishing term, and all the other terms vanish to at least second order. If we can find such a locus $\mathcal{Y}$, we can flow (as described in the previous paragraph) along that locus to a solution.

We find this desired locus by first considering the boundary $\partial\overline{\Delta}$ of the closure $\overline{\Delta}$ of the moduli space Δ: this boundary has strata of moduli spaces Δ' for minimal surface problems of lower complexity. Looking ahead to a proof by induction, we assume that there is a solution X' of those lower complexity (either genus or number of ends or both) problems represented on such a boundary strata Δ' (with all of the corresponding extremal lengths in agreement). Then we prove that there is a locus $\mathcal{Y} \subset \Delta$ inside the larger moduli space Δ (with $\mathcal{Y}$ limiting on X') which has the analogues of those same extremal lengths in agreement. As a corollary of that condition, the height function on $\mathcal{Y}$ has the desired simple properties.

This inductive step is a crucial part of the "handle addition" program. We are unable to see our way through the combinatorics of deforming the orthodisks at an arbitrary point $Z \in \Delta_g$, and so we restrict ourselves to a special sublocus built out of a lower genus solution.

Let us now explore some of the details of this step in the case of our example of the genus four surface E_4 with an end asymptotic to Enneper's surface. Here Δ_4 is a three-dimensional simplex bounded by four two-dimensional faces. Looking back at the figure Figure 9, we recognize that each of the boundary faces is represented by limits of orthodisks degenerating in a simple way: associate to each such boundary face, say $\mathcal{F}_i$, a finite edge, say E_i in the Figure 9. Then, consider a family of orthodisks in which the length of E_i is tending to zero, but the lengths of the other edges are converging to finite and positive numbers. This family converges to a point on $\mathcal{F}_i$, and we see that it is natural to parametrize $\mathcal{F}_i$ by the projectivization of the (positive and finite) lengths of the remaining edges. (We could then proceed to the faces of higher codimension in a similar manner, but this is not necessary for our purposes here.) We focus on the face $\mathcal{F}_1$ obtained by (symmetrically) collapsing the edges H_4H_5 and H_5H_6.

This face $\mathcal{F}_1$ parametrizes conjugate pairs for the problem of finding a genus three Enneper-ended surface E_3. We assume that there is such a solution, say X'.

At this less complex solution X' in the moduli space $\mathcal{F}_1 \subset \overline{\Delta}$, we aim to undo the degeneration which collapsed the two central edges to a point. In particular, we seek a path $\mathcal{Y} \subset \overline{\Delta}$ along which we retain the essential properties of X' that

$$\mathrm{Ext}_{\Gamma_2}(\Omega_{Gdh}) = \mathrm{Ext}_{\Gamma_2}(\Omega_{\frac{1}{G}dh}) \tag{4.3.17}$$

and

$$\mathrm{Ext}_{\Gamma_3}(\Omega_{Gdh}) = \mathrm{Ext}_{\Gamma_3}(\Omega_{\frac{1}{G}dh}). \tag{4.3.18}$$

Geometrically, we aim to "cut a small corner" into a lower genus pair of orthodisks, and then readjust the lengths of the larger sides so as to satisfy the conditions above. See Figure 25.

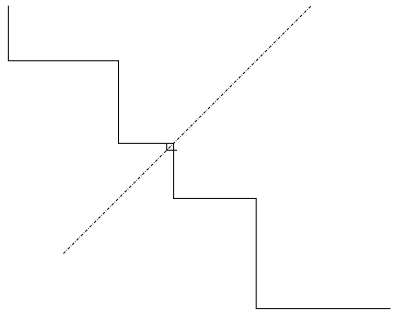

Figure 25: orthodisks for Gdh for E_4

By the implicit function theorem, to prove that this is possible, it is basically enough to show that X' is locally unique in the (finite dimensional) lower genus moduli space $\mathcal{F}_1$. But consider a deforming X' by, say, pushing an edge "into" Ω_{Gdh}. Thus we also push the corresponding edge "out of" $\Omega_{\frac{1}{G}dh}$.

Once again, we are comparing the flat geometries of Ω_{Gdh} and $\Omega_{\frac{1}{G}dh}$ to their underlying conformal geometries; this time our interest is in how a prescribed infinitesimal change in flat geometry (corresponding to a prescribed change in periods) affects the underlying conformal geometry. We study this using the standard calculus from Teichmüller theory [Ahl61]: tangent vectors to Teichmüller space are represented by Beltrami differentials, which are tensors of type $d\overline{z} \otimes \frac{\partial}{\partial z}$ that can be readily computed from a prescribed deformation of structure like the "pushing into" or "pushing out of" an edge. (See e.g. [WW] for full details.)

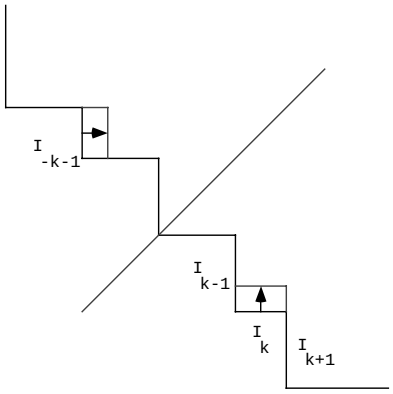

Figure 26: We push the k^{th} edge I_k and its reflection I_{-k-1} into Ω_{Gdh}

Formally then, the first operation of "pushing in" corresponds to an infinitesimal Beltrami differential $\dot{\mu}_G$ on Ω_{Gdh}, and the second operation of "pushing out" corresponds to an infinitesimal Beltrami differential $\dot{\mu}_{\frac{1}{G}}$ on $\Omega_{\frac{1}{G}dh}$. But as X' is a solution, we know that there is a *conformal* map $w : \Omega_{Gdh} \to \Omega_{\frac{1}{G}dh}$, and we can compute, using the tensor type of a Beltrami differential together with the fairly explicit "staircase-like" Euclidean geometry of Ω_{Gdh} and $\Omega_{\frac{1}{G}dh}$ (which then gives good control on the extension of w to $\partial\overline{\Omega_{Gdh}}$), that

$$w^*(\dot{\mu}_{\frac{1}{G}}) = -\dot{\mu}_G. \tag{4.3.19}$$

This equation (4.3.19) implies that any such deformation deforms the conformal structures of Ω_{Gdh} and $\Omega_{\frac{1}{G}dh}$ in *opposite* directions, where here by directions we mean as tangent vectors to appropriate Teichmüller spaces.

Remarks:

1) The Non-critical Flow/Regeneration inductive step seems quite general. Thus, in some sense, the most difficult period problem to solve is the low genus one. It is therefore significant that Horgan does not exist, as its existence might then have yielded existence of "k-handled Horgan".

2) We produced the face $\mathcal{F}_1$ by a process of allowing the orthodisks to degenerate: we (symmetrically) collapsed the middle edges H_4H_5 and H_5H_6 of the structures in Figure 9. On the surfaces obtained by taking a branched cover over the double of one of these structures, we would see lifts of the points H_4, H_5, and H_6 approaching one another (as measured in the flat metric) along such a degenerating family. Formally however, in terms of the underlying conformal structures, it does not make sense to speak of points coalescing on Riemann surfaces; it is only proper to speak of curves pinching off to form noded surfaces. (Noded surfaces are complex spaces where each neighborhood is either biholomorphic to a disk or biholomorphic to a domain $\{zw = t; |z| < \epsilon, |w| < \epsilon\}$ in $\mathbb{C}^2$. The complements of the nodes (where $z = w = 0$ above) are punctured Riemann surfaces, occasionally referred to as the regular components of the noded surface.) In the case of the Enneper-ended surfaces, since the limit of a degenerating family of

structures Ω_{Gdh} was a lower genus flat structure of the type Ω'_{Gdh}, we "see" only one regular component of the noded surface, as the limiting one-form on the other component is zero. This does not always hold in handle addition; for example in the Costa-type surfaces of [WW], the degenerate structures appear to be of the form of less complex structures, along with other very simple components. (See Figure 27 for the limit of a degenerating family of the form Figure 10.) The regeneration step is then more complex than the relatively simple "cutting of the corner" of Figure 25.

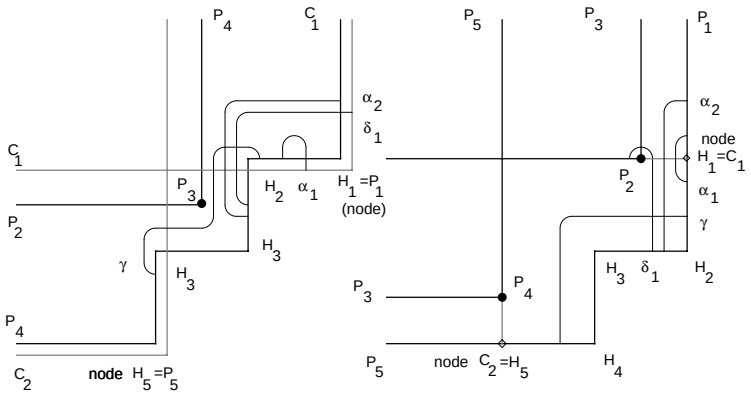

Figure 27: The limit of a family of degenerating surfaces of the type 10.

Here, on the right hand side, the regular components of the noded surface appear either as lower complexity orthodisks or as points, while on the left-hand side, the regular components which are not lower complexity orthodisks appear as non-trivial bigons

5 Beyond Enneper-ended Surfaces

We end with a few comments about the adjustments requred to adapt the outline above to the surfaces of the types in Theorems 1.0.3, 1.0.4 and 1.0.5, as well as deformations of those surfaces in continuous families. Basically, the above argument goes through relatively unchanged for the surfaces of Costa type. Of course, we need to choose the appropriate cycles and understand the impact of the orthodisks having several sheets, but then the Reflexivity and Properness proofs are identical to those for the Enneper-ended case. The discussion of Non-Critical Flow and Regeneration are a bit different however, as the degenerations of these orthodisks are different. In particular, when we regenerate, there are two parameters to add, and we need to always solve a 2-dimensional flow problem.

An interesting feature of this is that given a surface of type (m, n), we can choose to regenerate in either this two-parameter way, or in the way we discussed with respect to the Enneper-ended surfaces.

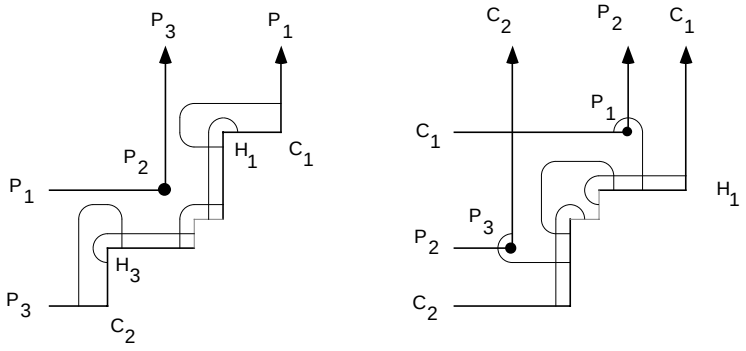

Figure 28: Regenerating orthodisks for $DH_{m,n}$, case $m < n$

This second method leads to surfaces like

Figure 29: The surface DH(1,2)

This represents how we fill in the superdiagonal entries in Table 1 described after Theorem 1.0.4.

Finally, we note that it is possible to deform the planar ends of the surfaces described in Theorem 1.0.4 into catenoid ends with specified growth rates near zero. A new type of special point is introduced into the orthodisk, but only mild modifications are required for the proofs.

References

[Ahl61] L. Ahlfors. Some remarks on teichmüller's space of riemann surfaces. *Ann. Math.*, 74:171–191, 1961.

[Ahl66] L. Ahlfors. *Lectures on Quasiconformal Mappings*. Van Nostrand, New York, 1966.

[BW] E. Boix and M. Wohlgemuth. Numerical results on embedded minimal surfaces of finite total curvature. In preparation.

[CG81] C. C. Chen and F. Gackstatter. Elliptic and hyperelliptic functions and complete minimal surfaces with handles. *Instituto de Matemática e Estatistica-Universidade de São Paulo*, 27, 1981.

[CG82] C. C. Chen and F. Gackstatter. Elliptische und Hyperelliptische Functionen und vollständige Minimalflächen von Enneperschen Typ. *Math. Ann.*, 259:359–369, 1982.

[CHMI89] M. Callahan, D. Hoffman, and W. H. Meeks III. Embedded minimal surfaces with an infinite number of ends. *Inventiones Math.*, 96:459–505, 1989.

[Cos84] C. Costa. Example of a complete minimal immersion in $\mathbb{R}^3$ of genus one and three embedded ends. *Bull. Soc. Bras. Mat.*, 15:47–54, 1984.

[Enn69] A. Enneper. Die cyklischen Flächen. *Z. Math. und Phys.*, 14:393–421, 1869.

[Gar87] F. Gardiner. *Teichmuller Theory and Quadratic Differentials*. Wiley Interscience, New York, 1987.

[HK97] D. Hoffman and H. Karcher. Complete embedded minimal surfaces of finite total curvature. In *Encyclopedia of Mathematics*, pages 5–93, 1997. R. Osserman, editor, Springer Verlag.

[HMI85] D. Hoffman and W. H. Meeks III. A complete embedded minimal surface in $\mathbb{R}^3$ with genus one and three ends. *Journal of Differential Geometry*, 21:109–127, 1985.

[HMI90] D. Hoffman and W. H. Meeks III. Embedded minimal surfaces of finite topology. *Annals of Mathematics*, 131:1–34, 1990.

[HW] D. Hoffman and F. Wei. Construction of a helicoid with a handle. Preprint.

[JI83] L. Jorge and W.H. Meeks III. The topology of complete minimal surfaces of finite total curvature. *Topology*, 22:203–221, 1983.

[Kar88] H. Karcher. Embedded minimal surfaces derived from Scherk's examples. *Manuscripta Math.*, 62:83–114, 1988.

[Kar89] H. Karcher. Construction of minimal surfaces. *Surveys in Geometry*, pages 1–96, 1989. University of Tokyo, 1989, and Lecture Notes No. 12, SFB256, Bonn, 1989.

[Kar91] H. Karcher. Construction of higher genus embedded minimal surfaces. In *Geometry and Topology of Submanifolds III (Leeds, 1990)*, pages 174–191, River Edge, NJ, 1991. World Sci. Publishing.

[MW01] F. Martin and M. Weber. On properly embedded minimal surfaces with three ends. *Duke Math. Journal*, 107:533–559, 2001.

[Oht70] M. Ohtsuka. *Dirichlet Problem, Extremal Length, and Prime Ends*. Van Nostrand Reinhold, New York, 1970.

[San94] N. Do Espirito Santo. Complete minimal surfaces with type enneper end. *Ann. Inst. Fourier (Grenoble)*, 44:525–577, 1994.

[Sat96] K. Sato. Existence proof of one-ended minimal surfaces with finite total curvature. *Tohoku Math. J.*, 48:229–246, 1996.

[Sch83] R. Schoen. Uniqueness, symmetry, and embeddedness of minimal surfaces. *Journal of Differential Geometry*, 18:791–809, 1983.

[Tha94] E. Thayer. *Complete Minimal Surfaces in Euclidean 3-Space*. PhD thesis, University of Massachusetts at Amherst, 1994.

[Web98] M. Weber. On the horgan minimal non-surface. *Calc. Var.*, 7:373–379, 1998.

[Web00] M. Weber. On singly periodic minimal surfaces invariant under a translation. *Manuscripta Mathematica*, 101:125–142, 2000.

[WW] M. Weber and M. Wolf. Teichmüller theory and handle addition for minimal surfaces. *Annals of Math.* to appear.

[WW98] M. Weber and M. Wolf. Minimal surfaces of least total curvature and moduli spaces of plane polygonal arcs. *Geom. and Funct. Anal.*, 8:1129–1170, 1998.

[WW01] M. Weber and M. Wolf. *Minimal Surfaces and Teichmueller Theory*. 2001. in preparation.